

Elsevier Editorial System(tm) for
Carbohydrate Polymers
Manuscript Draft

Manuscript Number: CARBPOL-D-18-00415R1

Title: Thermal conductivity, structure and mechanical properties of konjac glucomannan/starch based aerogel strengthened by wheat straw

Article Type: Research Paper

Keywords: konjac glucomannan; thermal insulation aerogel; wheat straw; starch; pore size distribution; mechanical property.

Corresponding Author: Professor Fatang Jiang, PhD

Corresponding Author's Institution: Hubei University of Technology

First Author: Yixin Wang

Order of Authors: Yixin Wang; Kao Wu; Man Xiao; Saffa B Riffat; Yuehong Su; Fatang Jiang, PhD

Abstract: This study presents the preparation and property characterization of a konjac glucomannan (KGM)/starch based aerogel as a thermal insulation material. Wheat straw powders (a kind of agricultural waste) and starch are used to enhance aerogel physical properties such as mechanical strength and pore size distribution. Aerogel samples were made using environmentally friendly sol-gel and freeze drying methods. Results show that starch addition could strengthen the mechanical strength of aerogel significantly, and wheat straw addition could decrease aerogel pore size due to its special micron-cavity structure, with appropriate gelatin addition as the stabilizer. The aerogel formula was optimized to achieve lowest thermal conductivity and good thermal stability. Within the experimental range, aerogel with the optimized formula had a thermal conductivity $0.04641 \text{ Wm}^{-1}\text{K}^{-1}$, a compression modulus 67.5 kPa and an elasticity 0.27. The results demonstrate the high potential of KGM/starch based aerogels enhanced with wheat straw and starch for application in thermal insulation.

1 **Thermal conductivity, structure and mechanical properties of konjac**
2 **glucomannan/**starch based** aerogel strengthened by wheat straw**

3

4 Yixin Wang^{1,2}, Kao Wu^{1,2}, Man Xiao^{1,2}, Saffa B.Riffat³, Yuehong Su^{3*} and Fatang
5 Jiang^{1,2,3*}

6 ¹Glyn O. Philips Hydrocolloid Research Centre at HUT, Hubei University of
7 Technology, Wuhan 430068, China;

8

9 ²School of Bioengineering and Food Science, Hubei University of Technology,
10 Wuhan 430068, China;

11

12 ³Department of Architecture and Built Environment, Faculty of Engineering,
13 University of Nottingham, University Park, Nottingham, NG7 2RD, UK

14

15 **Abstract:**

16 This study presents the preparation and property characterization of a konjac
17 glucomannan (KGM)/starch based aerogel as a thermal insulation material. Wheat
18 straw powders (a kind of agricultural waste) and starch are used to enhance aerogel
19 physical properties such as mechanical strength and pore size distribution. Aerogel
20 samples were made using environmentally friendly sol–gel and freeze drying methods.
21 Results show that starch addition could strengthen the mechanical strength of aerogel
22 significantly, and wheat straw addition could decrease aerogel pore size due to its
23 special micron-cavity structure, with appropriate gelatin addition as the stabilizer. The
24 aerogel formula was optimized to achieve lowest thermal conductivity and good
25 thermal stability. Within the experimental range, aerogel with the optimized formula
26 had a thermal conductivity $0.04641 \text{ Wm}^{-1}\text{K}^{-1}$, a compression modulus 67.5 kPa and an
27 elasticity 0.27. The results demonstrate the high potential of KGM/starch based
28 aerogels enhanced with wheat straw and starch for application in thermal insulation.

29 **Keywords:** konjac glucomannan; thermal insulation aerogel; wheat straw; starch;
30 pore size distribution; mechanical property.

31

32

33 Highlights:

34 1. Four natural raw materials were used for KGM/**starch** based aerogel preparation

35 2. KGM/**starch** based **aerogel** preparation via an energy **efficient** freeze drying
36 method.

37 **3. Starch was used to increase the mechanical strength of KGM/starch based aerogels.**

38 4. Wheat straw can improve thermal insulation by affecting pore structure.

39 5. Thermal insulation mechanism of KGM/**starch** based aerogel **was discussed.**

40

41

42 **1. Introduction**

43 Although people's living standards have been greatly improved with rapid economic
44 growth, the energy consuming level becomes much higher, raising considerable social
45 concerns about energy crisis and environmental problems. Currently energy
46 conservation and environmental protection have received growing attentions. To
47 reduce CO₂ emissions, numbers of low-energy buildings and passive houses have
48 been built in German (Beck, Heinemann, Reidinger, & Fricke, 2004). On the other
49 hand, a large amount of energy is used for space heating and air conditioning,
50 especially in extremely hot and cold climate regions, and the real estate has great
51 potential for energy saving by rational use of resources. According to this, the
52 European Union has set a goal for reductions in energy use and flue gas emissions
53 (Ramírez-Villegas, Eriksson, & Olofsson, 2016). Therefore, energy conservation
54 policy can be enforced and implemented by the development of thermal insulation
55 materials.

56

57 Commonly, thermal insulation materials are composed of organic polymers, such as
58 polyurethane foam, polystyrene foam, glass wool, etc. Polyurethane foam can be
59 divided into two categories: flexible polyurethane foam and rigid polyurethane foam
60 (Septevani, Evans, Chaleat, Martin, & Annamalai, 2015), and is often used as thermal
61 insulation materials in the building envelop and domestic refrigerators (Janik,
62 Sienkiewicz, & Kucinska-Lipka, 2014). However, the production of polyurethane
63 foam relies on the unsustainable petroleum sources, as its two main components are
64 isocyanates and polyether. Moreover, the widely use of polyurethane has produced

65 considerable amount of wastes, and these wastes usually go into landfill, which need
66 quite long time to be degraded. Possessing extremely low density and large surface
67 area, aerogel was invented by Kistler in 1931 (Kistler, 1931) and has also been used
68 as insulation material, e.g. in space suit and aerospace detector (Randall, Meador, &
69 Jana, 2011; Sabri, Marchetta, Faysal, Brock, & Roan, 2014). The heat transfer
70 mechanism of aerogel is explained by the combination of heat conduction in solid
71 backbone and gaseous phase and thermal radiation between the interior surfaces (Lee
72 & Cunnington, 2012; Lu, Caps, Fricke, Alviso, & Pekala, 1995). The effective total
73 thermal conductivity can be expressed as the solid thermal conductivity of the solid
74 backbone, the effective thermal conductivity of the gaseous phase, and-the radiative
75 heat exchange (Lee, Lee, Yim, Sun, & Yoo, 2002; Lu et al., 1995). Currently, most
76 aerogel materials are prepared from inorganic or petrochemical-based feedstock, such
77 as silica aerogels and resorcinol-formaldehyde aerogels (Mikkonen, Parikka, Ghafar,
78 & Tenkanen, 2013). However, the degradation time of these aerogels can be quite
79 long in nature and thus may cause harm to the environment. Therefore, alternative
80 new, green and sustainable polysaccharide-based aerogels have attracted a lot of
81 interests from researchers (Robitzer, Renzo, & Quignard, 2011).

82

83 As a renewable, sustainable, non-toxic material, polysaccharides including cellulose
84 (Thakur & Voicu, 2016), hemicellulose, marine polysaccharides, starch (Miculescu et
85 al., 2017), etc. have in common the ability to form gels in the presence of water or
86 with other cross-linking agents (He, Sui, He, & Li, 2015), and polysaccharide

87 aerogels with different physical, thermal, optical and acoustical properties (Wang,
88 Chen, Kuang, Jiang, & Yan, 2017) can be obtained by drying these gels through two
89 commonly used drying methods, supercritical drying and freezing drying. Protecting
90 structures from collapsing, the latter method, also known as lyophilization, is a
91 low-cost and convenient method preferred by industry consisting of moving frozen
92 water from a frozen sample by sublimation under vacuum. There have been a number
93 of reports on the preparation of polymer materials through freeze-drying process from
94 aqueous mixtures due to the safety and low cost (Wang, Alhassan, Yang, & Schiraldi,
95 2013), e.g. nanocellulose aerogel (Nemoto, Saito, & Isogai, 2015), biobased poly
96 (furfuryl alcohol) and clay aerogel (Wang, Sun, Long, Wang, & Schiraldi, 2016),
97 alginate nanocomposite aerogels (Ke et al., 2016).

98

99 Konjac glucomannan (KGM) is an abundant, nontoxic polysaccharide found in the
100 tuber of amorphophallus konjac plant. KGM is composed of glucose and mannose
101 linked by β -1, 4 glycosidic bonds at 1:1.5–1:1.6 molar ratio, with 5–10% acetyl
102 substitution (Davé & Mccarthy, 1997), and has high viscous property (30,000 mPa·s,
103 1%, w/v) and high molecular weight ($6.8 \times 10^5 \sim 9 \times 10^6$ Da) (Crosby, 2002). It can be a
104 good skeleton material for aerogel preparation based on our previous research (Ni et
105 al., 2016; Wang et al., 2017) . Wheat is cultivated in over 115 nations in the world,
106 producing a huge amount of straw as a byproduct. Wheat straw is usually treated by
107 incineration, causing serious air pollution to the environment. However, with its
108 special cavity structure, wheat straw can be also used as thermal insulation materials

109 (Beck et al., 2004; Palumbo, Avellaneda, & Lacasta, 2015). Gelatin and starch as
110 degradable natural materials can also be used for aerogel preparation (Chang, Chen, &
111 Jiao, 2010; García-González, Uy, Alnaief, & Smirnova, 2012; Kenar, Eller, Felker,
112 Jackson, & Fanta, 2014; Wang, J. et al., 2016). **Appropriate combination of different**
113 **polymers could contribute to significant improvements on material properties**
114 **(Corobea et al., 2016)**. According to previous research (Chen et al., 2017; Ni et al.,
115 2016; Wang et al., 2017), the pore structure and mechanical property of KGM-based
116 aerogels can vary a lot with different composition and formulae. Therefore, this study
117 aims to investigate the relationship between thermal insulation property and pore
118 structure of KGM/**starch** based aerogels enhanced with wheat straw and gelatin. The
119 impact of aerogel components on the mechanical property, thermal stability, density,
120 porosity of KGM/**starch** based aerogels was also studied. This research can contribute
121 to the development of biodegradable thermal insulation materials.

122

123 **2. Experiments**

124 **2.1 Materials**

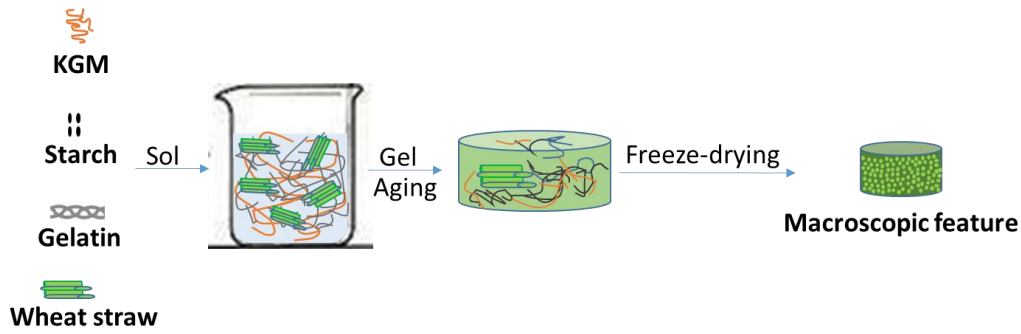
125 KGM was supplied by Licheng Biological Technology Co., Ltd. (Wuhan, China).
126 Potato starch was purchased from Wuhan Lin He Ji Food Co., Ltd. (Wuhan, China).
127 Gelatin was purchased from Sinopharm Chemical Reagent Co., Ltd. (Shanghai,
128 China). Raw wheat straw was obtained from Local farmers in Wuhan. After **being** cut
129 to small segments and washed more than 5 times, raw wheat straw was completely
130 dried in an oven at 90 °C. The **dried straw segments** was mechanically milled into
131 particles by a cereal pulverizer. Wheat straw powder were sieved through a 160 mesh

132 Tyler screen (pore size 94 μm) before being used.

133

134 **2.2 KGM/starch based aerogel preparation.**

135 The preparation of KGM/starch based aerogels was based on an invention patent of
136 Licheng Biological Technology in China (Jiang, 2013) as illustrated in Fig. 1. Gelatin
137 (0-1.5%, w/v) was first dissolved in double-distilled water (100 mL) in a water bath at
138 90 °C. Then KGM (0.5-1.5%, w/v), potato starch (1.0-3.0%, w/v) and wheat straw
139 powder (0.5-1.5%, w/v) were gradually added and mixed homogenously with the
140 stirring speed 600 rpm for 1 h to obtain the mixed sol. Subsequently the sol was
141 injected into a cylindrical 6 well cell culture cluster (diameter 34.8 mm and height 18
142 mm) and put into a 4 °C refrigerator for aging and molding for 2 h, before
143 immediately frozen in an ultra low temperature freezer (DW-FL262, Rowsen, China)
144 at -25 °C for 10 h. The frozen sample was dried in a freeze dryer (Modulyod-230,
145 Thermo Electron Corporation, USA) at -55 °C under a vacuum of 1 Pa for
146 approximately 24 h, and the aerogel (34.8 mm in diameter and about 10 mm in height)
147 was formed and obtained. All aerogel samples were coded in the form of
148 K0S0G0WS0 (K, S, G, WS represents konjac glucomannan, potato starch, gelatin,
149 wheat straw, respectively), and the number after K, S, G, WS indicates the weight
150 volume percent of composition in the original sol. Prior to tests, all samples were
151 stored in a dryer with silica gel beads and dried for 6 h at 60 °C in an oven.



153 **Fig. 1. Schematic procedure of preparing KGM/starch based aerogels**

154

155 **2.3 Characterization of KGM/starch based aerogels**

156 **2.3.1 Dry density**

157 The dry density (ρ) was calculated by the following equation:

158
$$\rho = \frac{m_0}{V}$$

159 Where m_0 is the dry weight of aerogel, V is the volume of the aerogel samples

160 **2.3.2 Estimation of porosity**

161 Porosity is an important structure parameter of KGM/starch based aerogel, and

162 porosity of aerogels was estimated according to Shi et al. (2013). Aerogel sample was

163 weighed first (m_0), then completely immersed in ethanol in a container and weighted

164 in total (m_1). The container was then put in a vacuum drying oven and vacuumized

165 until no air bubble coming out of the sample. After taking out the sample from the

166 container, the container with the residual ethanol was weighed (m_2). The porosity of

167 the sample can be calculated as below:

168
$$\text{Porosity (\%)} = \frac{\text{Weight of ethanol in sample}}{\text{Total weight of sample and ethanol}} = \frac{m_1 - m_2 - m_0}{m_1 - m_2} \times 100\%$$

169

170 **2.3.3 Morphology, microstructure and pore size distribution of KGM/starch**

171 **based aerogels**

172 The morphology and microstructure of **KGM/starch** based aerogels were observed
173 using SEM (JSM6390LV, JEOL, Tokyo, Japan). Prior to test, aerogel samples were
174 cut into 5 mm*5 mm*1 mm cubical pieces using a sharp razor blade. The cut surface
175 of samples were coated with gold particles (Bio-Rad type SC 502, JEOL Ltd, Japan)
176 by sputtering for 60 s, before observed at magnification of 50×, 150×, 500×, 1000×
177 using an accelerated voltage of 30 kV. Image Pro Plus software (Media Cybernetics
178 Inc, Maryland, America) was used to evaluate the pore size distribution of the
179 **KGM/starch** based aerogels based on 6 representative SEM images.

180

181 **2.3.4 Texture profile analysis**

182 The mechanical property of samples were tested by Texture analyzer (TA.XT Plus,
183 Stable Micro Systems, Surrey, UK) equipped with a 30 kg load cell and a discoidal
184 probe (d=100 mm, compression platen **Model No.** 10585) through double
185 compression tests. The test compression rate and ratio were 60 mm/min and 30%,
186 respectively, and the trigger force was set to 1.00 N in auto mode. The compressive
187 strength of specimens is defined as the maximum stress during the test. Sress (σ) was
188 calculated by the following standard equations:

$$189 \quad \sigma = \frac{F}{S_0}$$

190 where F is the force (in N) applied on the sample surface, S_0 in mm^2 , the initial
191 cross-sectional area of the sample.

192

193 **2.3.5 Thermal conductivity measurement**

194 Thermal conductivity of samples were measured at room temperature using a Thermal

195 Conductivity Analyzer (HOT DISK TPS2500, Uppsala, Sweden). The sensor
196 (polyimide sensor d=9.868 mm, Model No. 8563) are squeezed between two
197 KGM/starch based aerogel specimens. The equipment was put on a stable and flat
198 table with a heat shield. The core of the apparatus is a double spiral of thin nickel wire
199 (Gustafsson, 1991), which acts as the heat source controlling the temperature of the
200 sensor. An orthogonal design experiment was applied to investigate optimization of the
201 aerogel formula to minimize thermal conductivity. 4 factors (KGM, gelatin, starch,
202 wheat straw) and 3 levels (component concentration level) were selected according to
203 previous results.

204

205 **2.3.6 Thermogravimetric analysis (TGA)**

206 TGA was carried out to determine the thermostability by weight loss in relation to
207 temperature with a Netzsch TG 209 (Netzsch, Selb, Germany). The samples were
208 pulverized into granules by a pulverizer. With the nitrogen flow rate 20 mL/min, the
209 specimen was heated from 25 °C to 600 °C at heating rate 20 °C/min, and weight loss
210 curve was recorded.

211

212 **2.4 Statistical analysis**

213 All tests were performed at least in triplicate. Origin Pro 8 SR4 v8.0951 (OriginLab,
214 MA, USA) was used for figure drawing and linear regression analysis. SPSS (version
215 19, Endicott, NY, USA) was used for Pearson correlation analysis among porosity,
216 density, and thermal conductivity of aerogels.

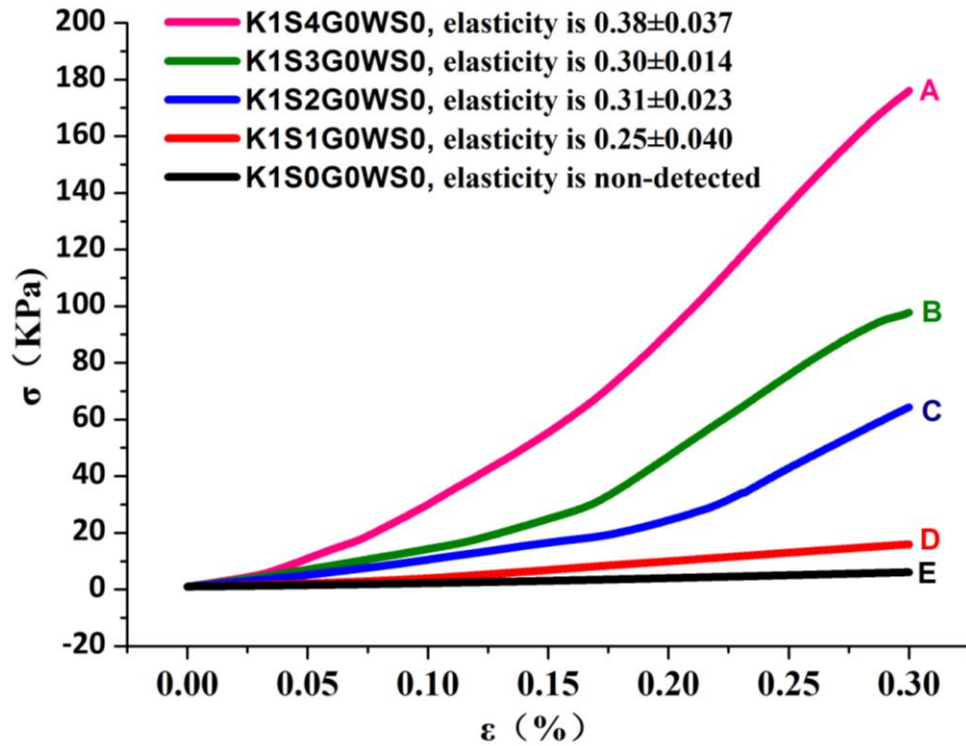
217

218 3. Results and discussion

219 3.1 Impact of starch on mechanical property of KGM-based aerogels

220 Generally, aerogels with higher compressive stress and elasticity are suggested for
221 practical applications. Representative stress-strain curves (strain 0-30%) for the effect
222 of starch concentration on the compressive strength are shown in Fig. 2. The
223 KGM-based aerogels had elasticity between 0.248 and 0.384. With starch
224 concentration 1%, the compressive strength of aerogel was improved slightly, and
225 starting from 2%, the compressive strength aerogel samples began to have significant
226 increase with the increase of starch concentration. The starch addition as the filler can
227 significantly improve the mechanical strength of the aerogels. There are two different
228 molecular components in starch, *i.e.*, amylose and amylopectin. Amylopectin
229 (molecular weight $\approx 10^8$ Da) contains a significantly higher branch density than
230 amylose (approximately 1% branch density, molecular weight $\approx 10^4$ to 10^6 Da).
231 Amylopectin is the major component in potato starch, and its branched structure could
232 endow the structural rigidity of starch, compared with KGM molecules which are
233 mostly linear chains without branches. Thus, starch presence could increase the
234 mechanical properties of KGM-based aerogel samples. To be more specific, compared
235 with K1S0G0WS0, starch addition of 1%, 2%, 3%, 4% can bring improvement of
236 stress by 161%, 956%, 1505%, 2788%, respectively.

237



238
 239 **Fig. 2. Stress-strain curves for KGM-based aerogels with different starch**
 240 **concentration**

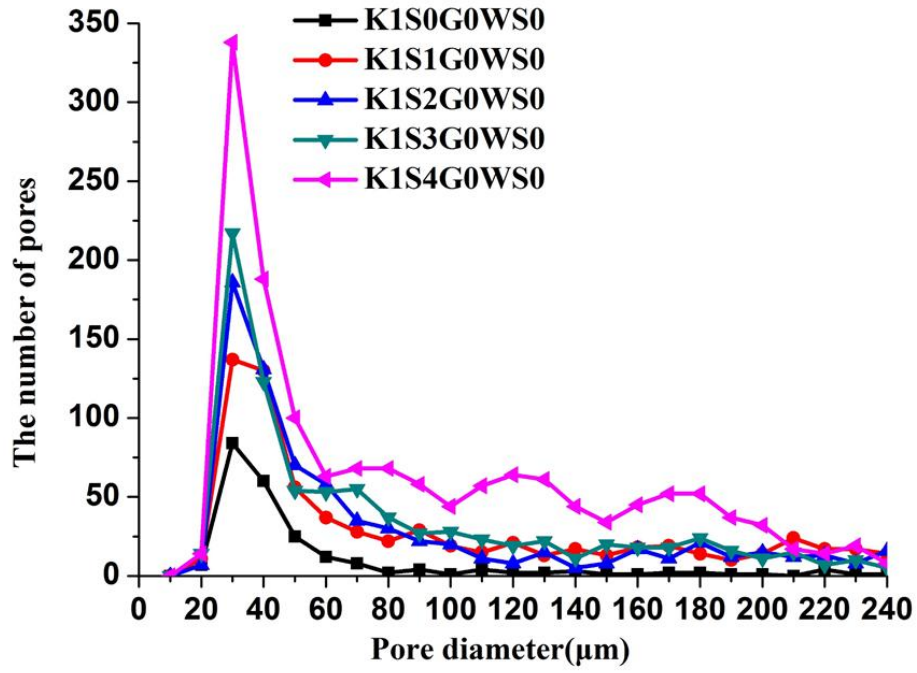
241 **3.2 Impact of starch and wheat straw on the structure of KGM-based aerogels**

242 Referring to our previous research (Ni et al., 2016), KGM-based aerogels pores are
 243 relatively big, spherical and uniform. With starch concentration increased from 0% to
 244 4% (w/v), the sum numbers of pores in aerogel with pore sizes 10-50 μm were
 245 gradually increased (Fig. 3A, B). Moreover, a good linearity ($R^2 = 0.9240$) was
 246 observed between the sum number of pores and the starch concentration (Fig. 3C).
 247 This suggests that by varying starch concentration, the pore size of aerogels could be
 248 adjusted to desired value through a linear model. With increased starch concentration,
 249 the pore walls became thicker, and the pore channel size decreased. This would
 250 benefit formation of close pores in aerogels, improving thermal insulation property
 251 (Wang, Zhong, Wang, & Yu, 2006). However, too high starch concentration may lead
 252 to very high density of aerogels, and this does not benefit the thermal insulation

253 capability. Therefore, starch concentration of 2% (w/v) was preliminarily selected in
254 the following parts, as it could already significantly improve the compressive stress
255 and pore size, compared with pure KGM aerogel (K1S0G0WS0).

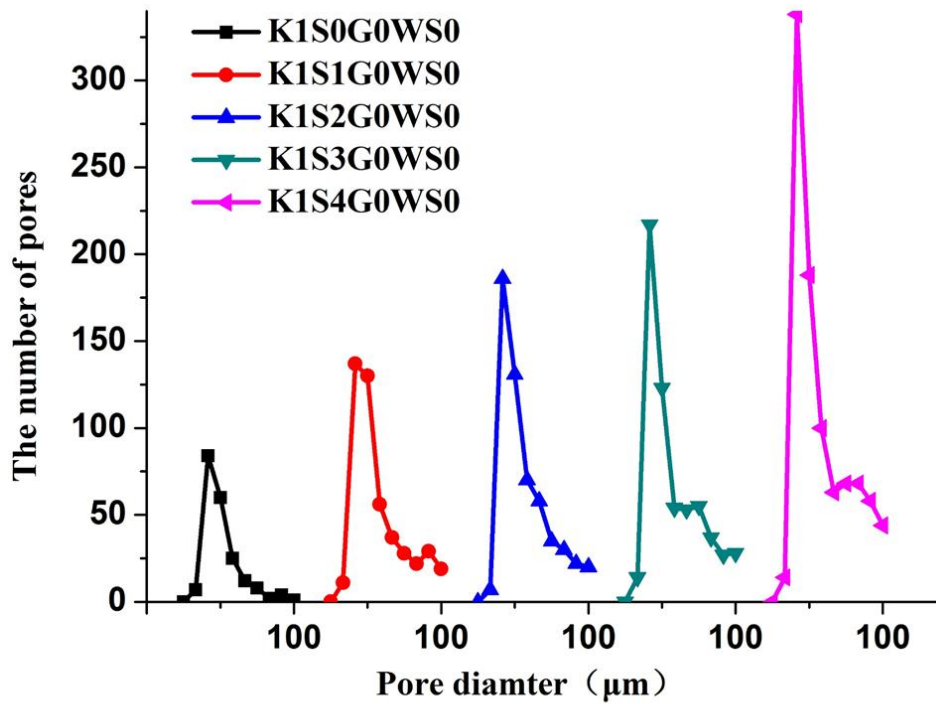
256

257 After wheat straw addition, the obtained KGM/starch based aerogels showed a
258 greenish brown appearance with flat smooth parallel surface (Fig. 4a). Wheat straw
259 has multi-cavities (Fig. 4b, c), and therefore with different wheat straw addition, the
260 pore size distribution of KGM-based aerogels are adjusted, and thermal insulation
261 properties can be changed. All KGM-based aerogels (Fig. 4d-i) had three-dimensional
262 network structure. Without wheat straw addition, pores were almost round (Fig. 4d),
263 and after wheat straw addition, the pores were smaller and their shapes was changed
264 from polygons into irregular shape (Fig. 4e). This may be explained by that the wheat
265 straw addition caused shape changes of ice crystal formed during freezing, which
266 could affect the distribution of pore size, the shape and the connectivity of the porous
267 network (Kiani & Sun, 2011). Besides, wheat straw can also provide many
268 micron-scale pores due to their multi-cavities, and this was supported by the size
269 distribution results of aerogel pores (Fig. 3D), as K1S2G0WS1.5 had much more
270 numbers of smaller pores than K1S2G0WS0. Without wheat straw (K1S2G0WS0),
271 the wave crest (10-50 μm) pores in aerogel was found to include only 48.83% of the
272 total number (806) of pores, and when wheat straw was added, a slight spike (10-50
273 μm) appeared covering 66.98% of the total number (966) of aerogel pores. Therefore,
274 with wheat straw addition, the pore size was significantly decreased (Fig. 4).



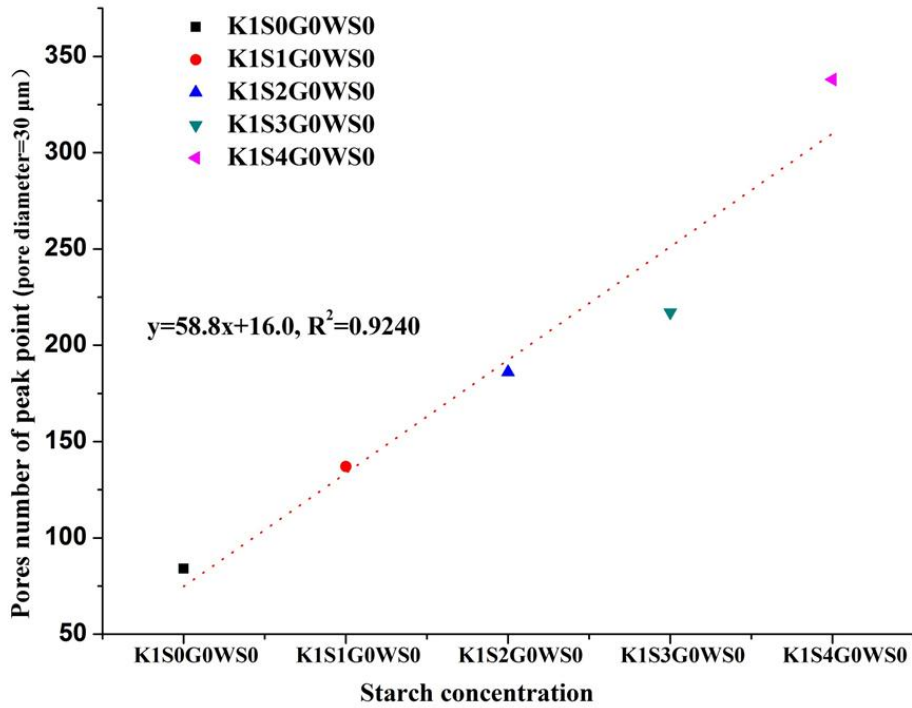
275

A



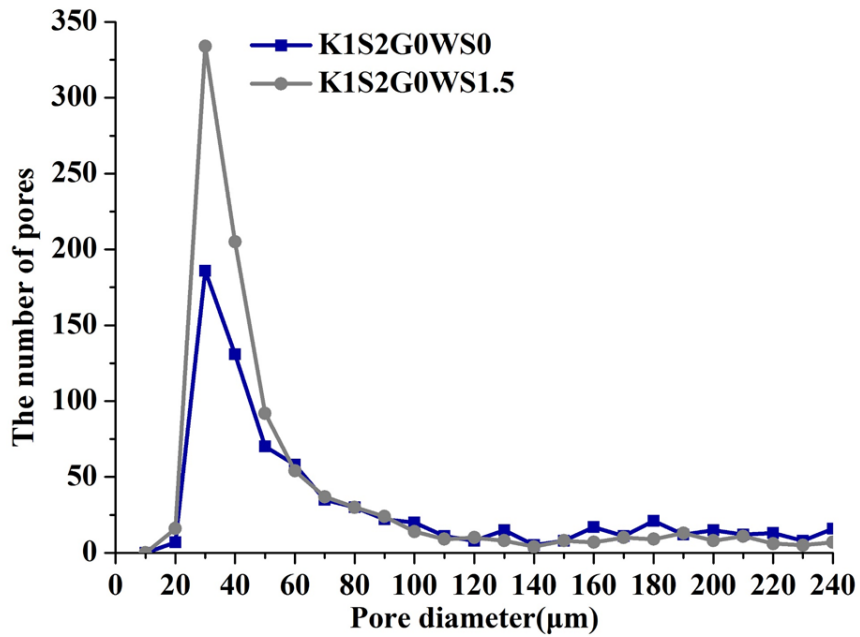
276

B



C

277



D

278

279

280

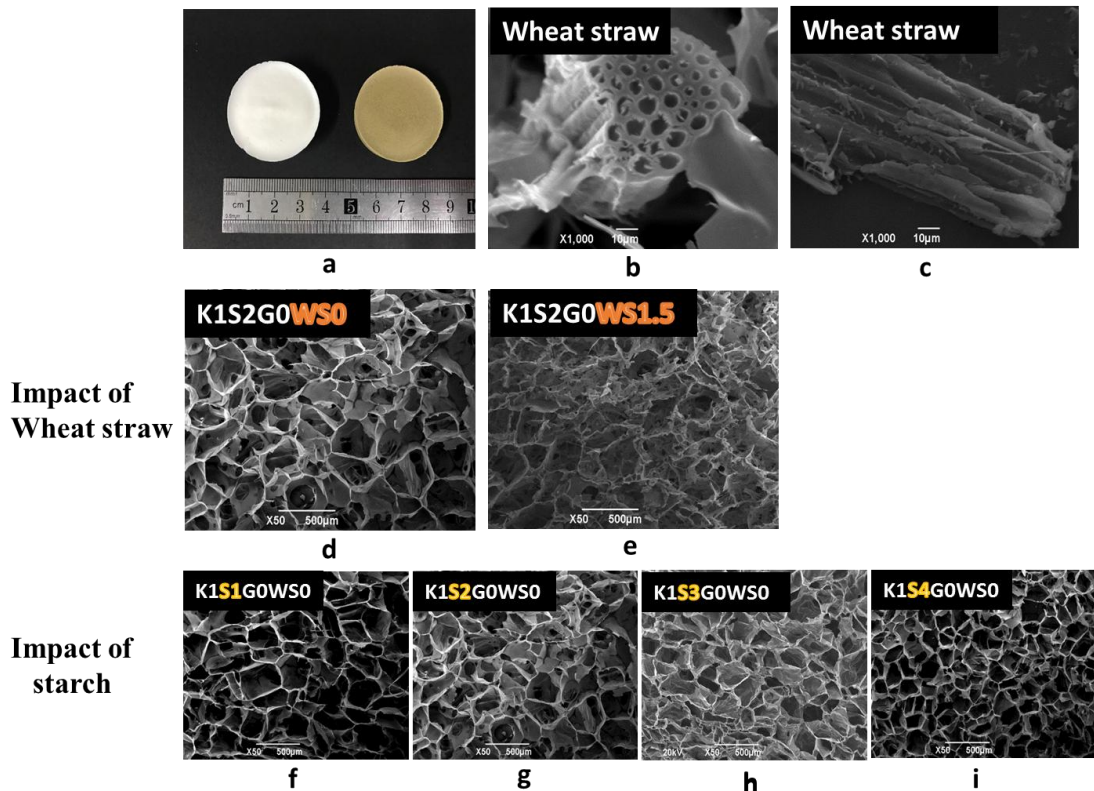
281

282

283

284

Fig. 3. (A, B) Size distribution (A: 0-240 μm; B: 0-100μm) of KGM-based aerogels pores with different starch concentration; (C) Linear relationship between starch concentration and aerogel pore numbers at pore diameter 30 μm; (D) Size distribution of KGM-based aerogels pores with different wheat straw concentration



285

286 **Fig. 4. Images of KGM-based aerogels with and without wheat straw (a), wheat**
 287 **straw (b, c) and SEM observations of KGM-based aerogels (d-i)**

288

289 3.3 Thermal insulation property

290 3.3.1 General heat transfer analysis for KGM/**starch** based aerogels.

291 The effective total thermal conductivity can be expressed as the sum of solid thermal

292 conductivity of the solid backbone, the effective thermal conductivity of the gaseous

293 phase, and the radiative conductivity. For KGM/**starch** based aerogel, the heat transfer

294 mechanism mainly include the solid conduction through the aerogel skeleton and the

295 gas conduction in the pores. According to this, the thermal insulation property is

296 related to the pores size distribution, pore shape, and pore walls. The solid backbone

297 of aerogels were composed of different materials whose volume heat capacity,

298 frequency-averaged mean free path of phonons and average phonons velocity are

299 invariable. However, solid conduction correlates with density which can be changed

300 by the concentration of raw materials, and the higher ρ , the higher solid heat

301 conduction λ_s . Low-density porous materials can have superinsulation properties as a
302 result of the air confined in their pores when the pore size is below the free mean path
303 of air molecules. Therefore, smaller average pore size of KGM/starch based aerogel
304 should be preferred in order to achieve lower thermal conductivity, and this can also
305 reduce the occurrence of open pores, which will benefit restricting gaseous heat
306 transfer.

307

308 3.3.2 Thermal conductivity of KGM/starch based aerogels

309 Though wheat straw addition (1.5%, w/v) could improve aerogel pore size
310 distributions, however, wheat straw subsidence occurred sometimes due to shear
311 thinning phenomenon. As gelatin solution was found to convert into gel rapidly after
312 the temperature was decreased to below 37 °C (Liu & Ma, 2009), it was further
313 introduced to keep wheat straw from subsiding. We had designed a single-factor
314 experiment to investigate the impact of gelatin on KGM-based aerogels, and the
315 results indicated that higher gelatin addition would contribute to irregular
316 macroscopic feature with more through-holes, which would lead to negative effect on
317 thermal insulation (Fig. S1). However, a small number of gelatin can avoid the wheat
318 straw from subsiding and can keep wheat straw evenly dispersive, and therefore a
319 critical and small gelatin addition would benefit the aerogel preparation.

320

321 Based on the above results and discussion, a L9 (3⁴) orthogonal array test was
322 performed to analyze the impact of different components and concentrations on the
323 thermal conductivity and to obtain the optimized aerogel formula. Four factors (four

324 different raw materials: KGM, starch, gelatin, and wheat straw) and three levels (three
325 different concentration) were applied, and 9 different aerogel samples were selected
326 (Table 1). Significant thermal conductivity differences were observed among different
327 samples. K1.0S2.0G0WS1.5 showed the lowest thermal conductivity (0.04683
328 $\text{Wm}^{-1}\text{K}^{-1}$), and K1.5S2.0G1.0WS0.5 had the highest ($0.05329\text{Wm}^{-1}\text{K}^{-1}$). Based on the
329 thermal conductivity values of the 9 designed samples, k and Range values were
330 calculated and the results indicated the effect of raw material concentration on the
331 thermal conductivity followed the order: gelatin > wheat straw > starch > KGM,
332 according to the values of range. The optimized aerogel formula was therefore
333 calculated to be K1S2G0.5WS1.5. To confirm this, we had prepared aerogel sample
334 K1S2G0.5WS1.5, and its thermal conductivity was measured to be $0.04641\text{Wm}^{-1}\text{K}^{-1}$,
335 a little lower than K1S2G0WS1.5. Its compressive strength, elasticity were 80.5 kPa,
336 0.273, respectively. This thermal insulation orthogonal test result was also in
337 accordance with the previous discussion in mechanical property section where 2 %
338 (w/v) starch addition was preliminarily selected. With more starch concentration, the
339 thickness of pore walls was increased and so was the solid phase heat conduction.

340

341 Porosity, density are important factors affecting thermal conductivity. The density and
342 porosity of all samples are shown in Table 2. Pearson correlation analysis showed that
343 density and porosity had strong negative relationship (Pearson coefficient= -0.799,
344 $p<0.01$), and both of them did not have significant relationships with thermal
345 conductivity ($p>0.05$). This was in agreement with most previous researchers who

346 found that single relationship between thermal conductivity and porosity could hardly
347 be established, because not only the volume pore fraction but also the other factors
348 such as pore size, shape, density and orientation can impact thermal conductivity
349 (Francl & Kingery, 1954). In the same time, the gaseous (λ_g) and the radiative (λ_r)
350 conductivities reduce along with the density which relates to solid content, while the
351 solid conductivity increase with the density (Lu et al., 1995). The thermal
352 conductivity differences of KGM/starch based aerogels may have to be explained
353 from the pore size and structure analysis.

354

355 From the samples listed in Table 1 and 2, we selected two aerogel samples with low
356 thermal conductivity (K1S2G0WS1.5, K1S2G0.5WS1.5) and K1S2G0WS0 to
357 analysis the impact of pore structure on thermal conductivity. Compared with
358 K0.5S1G0WS0.5 which had lowest density, K1S2G0WS1.5 had smaller pores (Fig.
359 5), leading to lower values of λ_s and λ_g . K1S2G0WS1.5 may be composed of more
360 closed pores with main pore size distribution about 30 μm . Compared with
361 K1S2G0WS0, the pore wall surface of K1S2G0WS1.5 was unsmooth with some
362 linear cavity structure which make the connectivity of the porous network more
363 complex (Fig. 4e), due to the impact of wheat straw addition. Moreover, after adding
364 wheat straw powder, gaseous flow path may have been changed to be more
365 complicated leading to the lower thermal conductivity. Additionally, with many
366 micron-scale pores, wheat straw addition could make aerogel pores (Fig. 5e, f)
367 become more complicated which was good thermal insulation due to elongated heat

368 transfer path. Compared with K1S2G0WS1.5, the optimized formula
 369 K1S2G0.5WS1.5 had only the differences of small amount of gelatin addition, and
 370 this resulted in further lower thermal conductivity. This may be explained by that
 371 wheat straw was more evenly distributed in K1S2G0.5WS1.5. Additionally, as air had
 372 low thermal conductivity ($0.0267 \text{ Wm}^{-1}\text{K}^{-1}$), the higher porosity of
 373 K1S2G0.5WS1.5 may also contribute to its lowest thermal conductivity.

374

375 **Table 1. Analysis of $L_9(3)^4$ test results**

Sample code	KGM	Starch	Gelatin	Wheat straw	Thermal Conductivity
	(g/100mL)				(Mean \pm SD)
K0.5S1.0G0WS0.5	0.5	1.0	0	0.5	0.05147 \pm 0.00050
K0.5S2.0G0.5WS1.0	0.5	2.0	0.5	1.0	0.04870 \pm 0.00030
K0.5S3.0G1.0WS1.5	0.5	3.0	1.0	1.5	0.05275 \pm 0.00066
K1.0S2.0G0WS1.5	1.0	2.0	0	1.5	0.04683 \pm 0.00178
K1.0S3.0G0.5WS0.5	1.0	3.0	0.5	0.5	0.05166 \pm 0.00012
K1.0S1.0G1.0WS1.0	1.0	1.0	1.0	1.0	0.05135 \pm 0.00066
K1.5S3.0G0WS1.0	1.5	3.0	0	1.0	0.05163 \pm 0.00012
K1.5S1.0G0.5WS1.5	1.5	1.0	0.5	1.5	0.04852 \pm 0.00178
K1.5S2.0G1.0WS0.5	1.5	2.0	1.0	0.5	0.05329 \pm 0.00017
k1	0.05098	0.05051	0.05004	0.05214	
k2	0.04995	0.04961	0.04957	0.05056	
k3	0.05114	0.05195	0.05246	0.04937	

Range	0.00120	0.00235	0.00290	0.00278
Optimal level	G>WS>S>KGM			
Major factor	1%	2%	0.5%	1.5%

Optimized formula

K1S2G0.5WS1.5

0.04641±0.00007

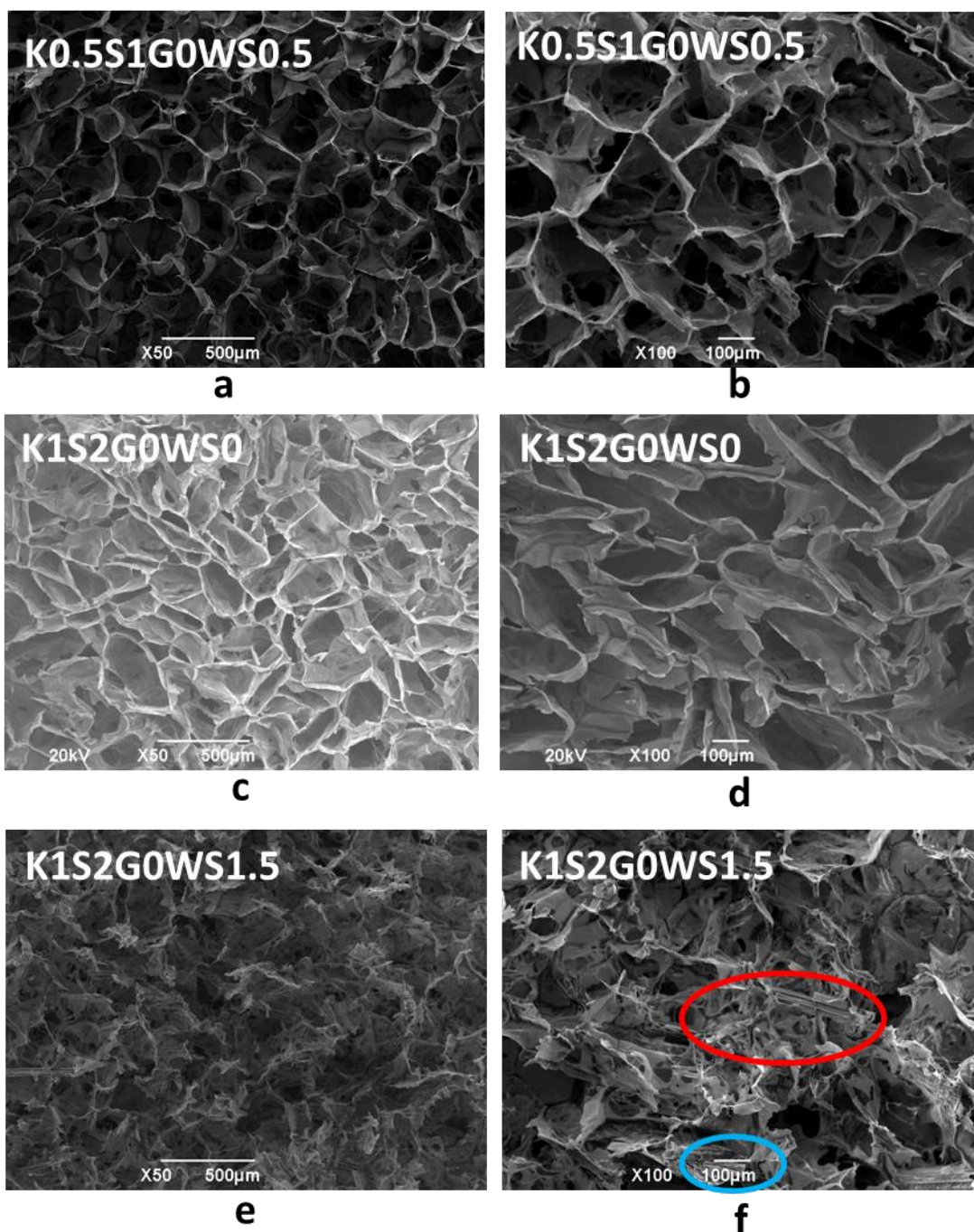
376 Range refers to the result of extreme analysis, Range = max {k1, k2, k3} – min {k1, k2, k3}. Where ki (i=1, 2,

377 3) represent the corresponding mean value of thermal conductivity at each level of concentration.

378 **Table 2. Aerogels of different composition and their porosity and density testing**
 379 **results**

Sample	Porosity (%)	Density(g/cm ⁻³)
K0.5S1.0G0WS0.5	97.17±0.03	0.0201±0.0002
K0.5S2.0G0.5WS1.0	93.76±0.09	0.0410±0.0006
K0.5S3.0G1.0WS1.5	94.28±0.08	0.0524±0.0015
K1.0S2.0G0WS1.5	93.28±0.06	0.0409±0.0013
K1.0S3.0G0.5WS0.5	92.65±0.05	0.0506±0.0001
K1.0S1.0G1.0WS1.0	94.43±0.04	0.0358±0.0010
K1.5S3.0G0WS1.0	92.49±0.07	0.0471±0.0015
K1.5S1.0G0.5WS1.5	93.80±0.05	0.0392±0.0006
K1.5S2.0G1.0WS0.5	94.40±0.02	0.0437±0.0008
K1S2G0.5WS1.5(Optimized formula)	94.50±0.03	0.0433±0.0002

380



381

382 **Fig. 5. SEM of Samples K0.5G0S1WS0.5 and K1S2 G0WS0 and SEM**
 383 **of Sample K1S2G0WS1.5 under different magnification 50X, 100X.**

384

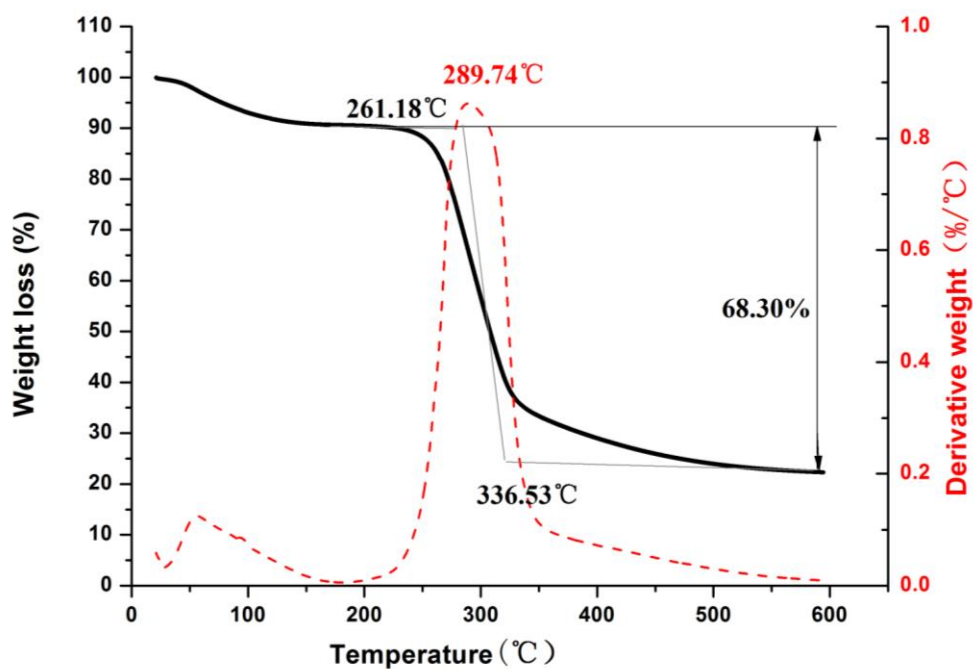
385 3.4 Thermogravimetric analysis

386 TG curves (**Fig. 6**) and detailed data in supplementary materials (**Table S1**) indicated

387 that KGM/starch based aerogels were decomposed in two steps. The first stage of

388 mass loss at around 100 °C in all samples corresponded to the dehydration, indicating

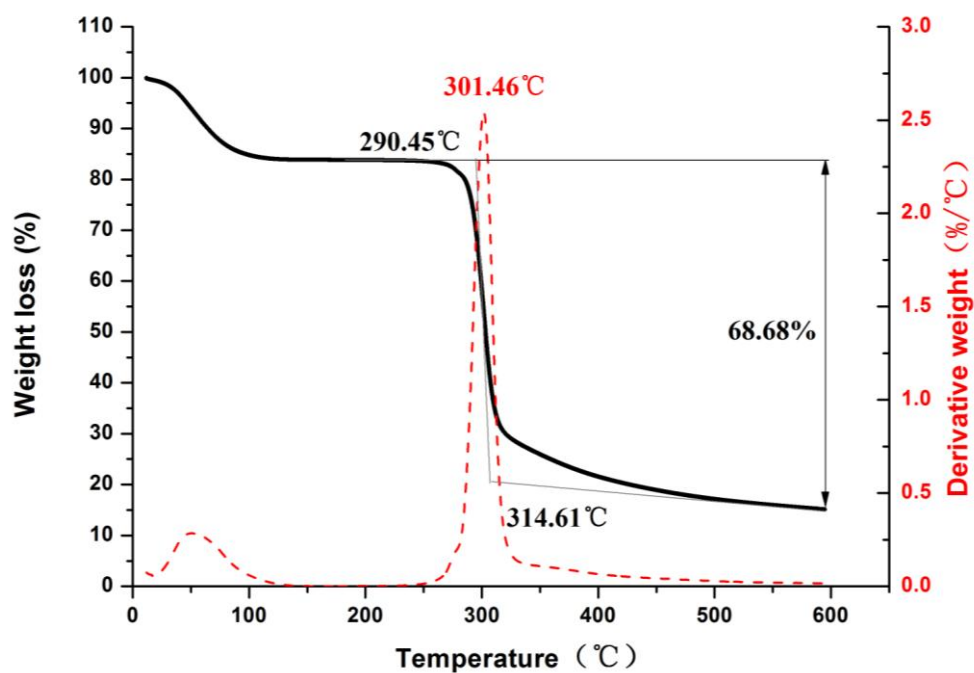
389 some moisture was still present in samples. This may be caused by the porous
390 structure and hydrophilic nature of KGM/**starch** based aerogels, which **could adsorb**
391 moisture from the air. The second stage of mass loss should be accredited to the
392 pyrolysis of polysaccharide and protein, reflecting thermal stability. All sample
393 showed similar mass loss ($\approx 68\%$) during the decomposition stage. As the framework
394 material of aerogels, KGM had a decomposition temperature from 261.18 to
395 336.53 °C, lower than wheat straw, gelatin and starch. The mass loss stage for
396 K1S2G0WS1.5 was from 272.62 to 344.38 °C, where around 70.90% weight was lost
397 due to the degradation of the polysaccharide, protein and wheat straw. It can be seen
398 that the thermal stability of KGM/**starch** based aerogel was between the properties of
399 four pure components. At 302.98 °C, K1S2G0WS1.5 had the maximum thermal
400 decomposition rate.



401

402

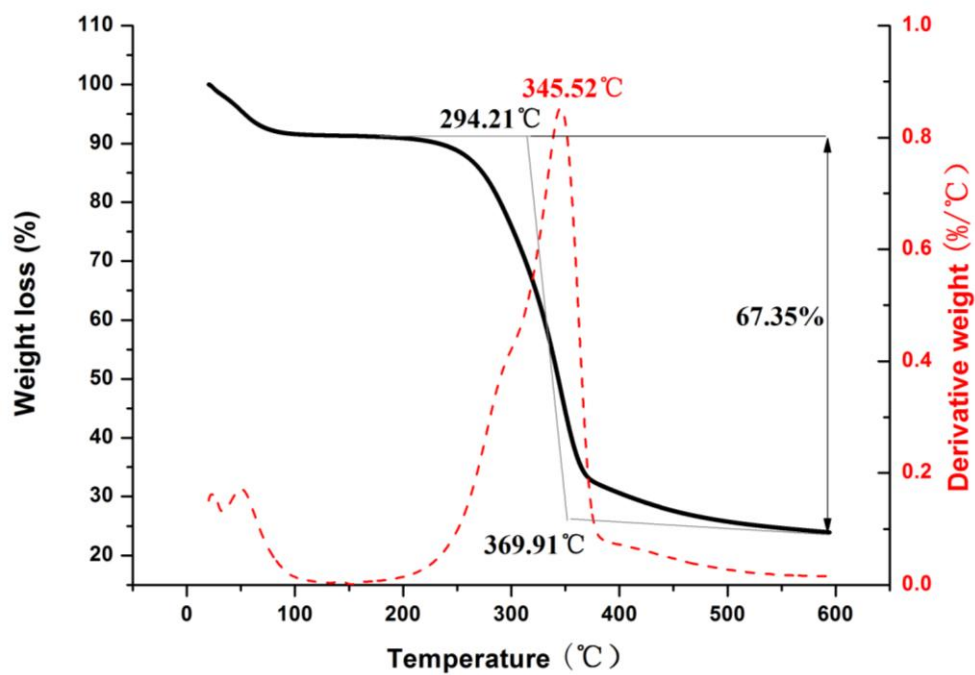
(a) KGM



403

404

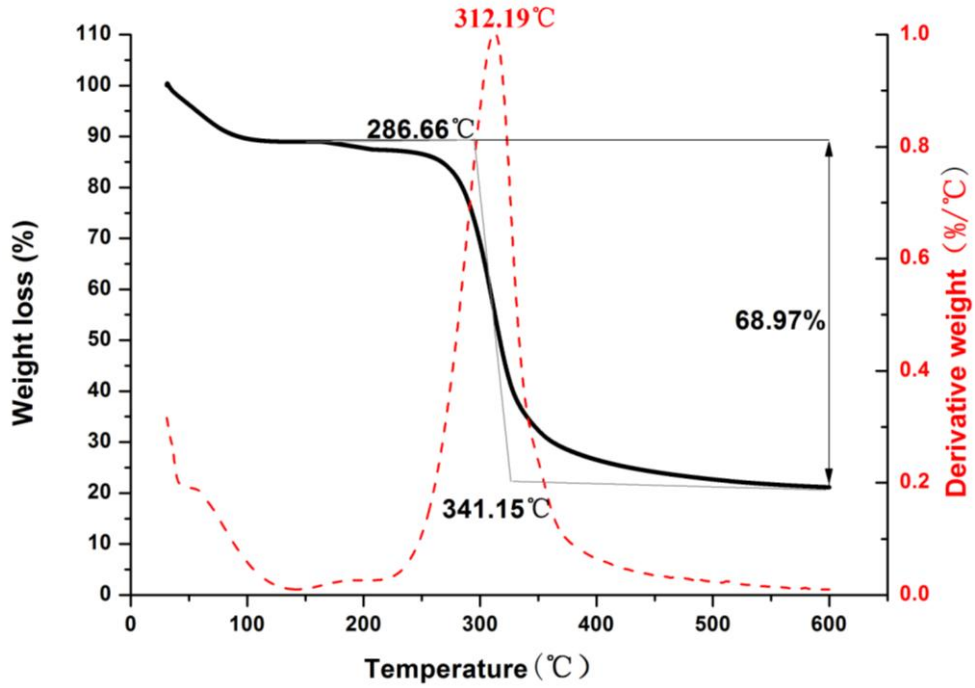
(b) Starch



405

406

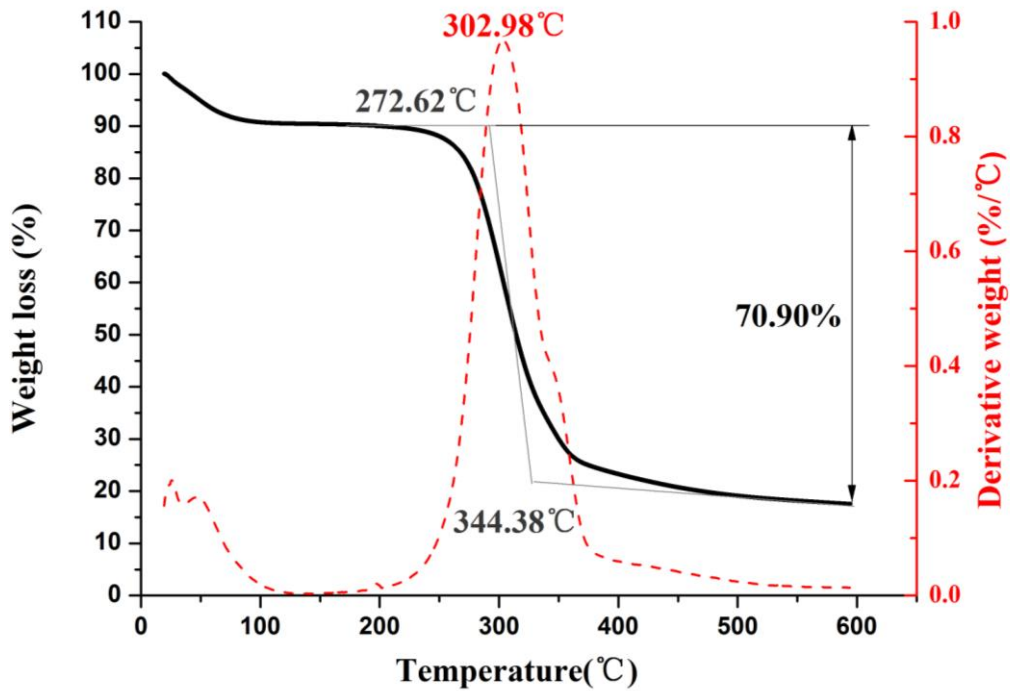
(c) Wheat straw



407

408

(d) Gelatin



409

410

(e) K1S2G0WS1.5

Fig. 6. TGA of pure raw materials and KGM/starch based aerogel

412

4. Conclusions

414 KGM/starch based aerogels have been prepared via a convenient, energy-efficiency

415 freeze drying method. The thermal conductivity of KGM/starch based aerogels has
416 been determined to be 0.046-0.053 Wm⁻¹K⁻¹. The optimized KGM/starch based
417 aerogel sample for thermal insulation was determined to be K1S2G0.5WS2, with its
418 thermal conductivity 0.04641Wm⁻¹K⁻¹, density 0.043g/cm⁻³, porosity 94.50±0.0291%,
419 compressive strength 80.5kPa and elasticity 0.273. The effect of different aerogel
420 components and their concentration on the mechanical property, porosity, density,
421 insulation property, thermal stability, pore size distribution and structure of aerogels
422 has been investigated. Starch can influence mechanical property, pore size, and pore
423 wall thickness of aerogels. Wheat straw can strengthen the thermal insulation property
424 of KGM/starch based aerogels due to the special cavity structure of wheat straw
425 affecting aerogel pore structure and decreasing pore size. Small amount of gelatin
426 addition is necessary to prevent wheat straw subsiding during aerogel preparation and
427 can also improve thermal insulation property. Thermal decomposition properties of
428 KGM/starch based aerogels fall between the values of their raw materials. This study
429 presents a way to manufacture aerogel from natural polysaccharide materials with a
430 satisfactory thermal insulation property.

431

432

433 **Acknowledgement**

434 This work is financially supported by the European Commission for the **MARIE**
435 **SKŁODOWSKA-CURIE** individual Fellowship grant (project ID: 794680), National
436 Natural Science Foundation of China (Grant No. 31671827) and the technology
437 support program of Hubei Science and Technology Department (No. 2016ACA164)

438

439

440 **References**

- 441 Beck, A., Heinemann, U., Reidinger, M., & Fricke, J. (2004). Thermal transport in
442 straw insulation. *Journal of Building Physics*, 27(27), 227-234.
- 443 Chang, X., Chen, D., & Jiao, X. (2010). Starch-derived carbon aerogels with
444 high-performance for sorption of cationic dyes. *Polymer*, 51(16), 3801-3807.
- 445 Chen, X., Kuang, Y., Xiao, M., Wu, K., Yan, W., Jiang, F., & Huang, J. (2017). Study
446 on adsorption of plant polysaccharide aerogels. *Science and Technology of*
447 *Food Industry*, 38(11).
- 448 Corobea, M. C., Muhulet, O., Miculescu, F., Antoniac, I. V., Vuluga, Z., Florea, D., . . .
449 Voicu, S. I. (2016). Novel nanocomposite membranes from cellulose acetate
450 and clay - silica nanowires. *Polymers for Advanced Technologies*, 27(12),
451 1586-1595.
- 452 Crosby, G. (2002). Managing healthy levels of blood glucose and cholesterol with
453 konjac flour. *Special Publication- Royal Society of Chemistry*, 278, 338-341.
- 454 Davé, V., & McCarthy, S. P. (1997). Review of konjac glucomannan. *Journal of*
455 *environmental polymer degradation*, 5(4), 237.
- 456 **Francl, J., & Kingery, W. D. (1954). Thermal Conductivity: IX, Experimental**
457 **investigation of effect of porosity on thermal conductivity. *Journal of the***
458 ***American Ceramic Society*, 37(2), 99-107.**
- 459 García-González, C. A., Uy, J. J., Alnaief, M., & Smirnova, I. (2012). Preparation of
460 tailor-made starch-based aerogel microspheres by the emulsion-gelation
461 method. *Carbohydrate Polymers*, 88(4), 1378-1386.
- 462 Gustafsson, S. E. (1991). Transient plane source techniques for thermal conductivity
463 and thermal diffusivity measurements of solid materials. *Review of Scientific*
464 *Instruments*, 62(3), 797-804.
- 465 He, F., Sui, C., He, X., & Li, M. (2015). Facile synthesis of strong alumina-cellulose
466 aerogels by a freeze-drying method. *Materials Letters*, 152, 9-12.
- 467 Janik, H., Sienkiewicz, M., & Kucinska-Lipka, J. (2014). 9 - Polyurethanes. In
468 *Handbook of thermoset plastics (Third Edition)* (pp. 253-295). Boston:
469 William Andrew Publishing
- 470 Jiang, F. (2013). Plant polysaccharide cigarette filter tip and preparation method
471 thereof. (**Pattern NO. 102423132**). CN.
- 472 Ke, S., Wang, L., Wang, J., Wang, Y. T., Wang, Y. Z., & Schiraldi, D. A. (2016).
473 Non-flammable alginate nanocomposite aerogels prepared by a simple freeze
474 drying and post-crosslinking method. *ACS Applied Materials & Interfaces*,
475 8(1), 643.
- 476 Kenar, J. A., Eller, F. J., Felker, F. C., Jackson, M. A., & Fanta, G. F. (2014). Starch
477 aerogel beads obtained from inclusion complexes prepared from high amylose
478 starch and sodium palmitate. *Green Chemistry*, 16(4), 1921-1930.
- 479 Kiani, H., & Sun, D. W. (2011). Water crystallization and its importance to freezing of
480 foods: A review. *Trends in Food Science & Technology*, 22(8), 407-426.
- 481 Kistler, S. S. (1931). Coherent expanded aerogels and jellies. *Nature*, 127, 741.
- 482 Lee, O. J., Lee, K. H., Yim, T. J., Sun, Y. K., & Yoo, K. P. (2002). Determination of

483 mesopore size of aerogels from thermal conductivity measurements. *Journal*
484 *of Non-Crystalline Solids*, 298(2–3), 287-292.

485 Lee, S., & Cunnington, G. R. (2012). Conduction and radiation heat transfer in
486 high-porosity fiber thermal insulation. *Journal of Thermophysics & Heat*
487 *Transfer*, 14(2), 121-136.

488 Liu, X., & Ma, P. X. (2009). Phase separation, pore structure, and properties of
489 nanofibrous gelatin scaffolds. *Biomaterials*, 30(25), 4094.

490 Lu, X., Caps, R., Fricke, J., Alviso, C. T., & Pekala, R. W. (1995). Correlation
491 between structure and thermal conductivity of organic aerogels. *Journal of*
492 *Non-Crystalline Solids*, 188(3), 226-234.

493 Miculescu, F., Maidaniuc, A., Voicu, S. I., Thakur, V. K., Stan, G. E., & Ciocan, L. T.
494 (2017). Progress in Hydroxyapatite–Starch Based Sustainable Biomaterials for
495 Biomedical Bone Substitution Applications. *ACS Sustainable Chemistry &*
496 *Engineering*, 5(10).

497 Mikkonen, K. S., Parikka, K., Ghafar, A., & Tenkanen, M. (2013). Prospects of
498 polysaccharide aerogels as modern advanced food materials. *Trends in Food*
499 *Science & Technology*, 34(2), 124-136.

500 Nemoto, J., Saito, T., & Isogai, A. (2015). Simple freeze-drying procedure for
501 producing nanocellulose aerogel-containing, high-performance air filters. *Acs*
502 *Applied Materials & Interfaces*, 7(35), 19809-19815.

503 Ni, X., Ke, F., Xiao, M., Wu, K., Kuang, Y., Corke, H., & Jiang, F. (2016). The control
504 of ice crystal growth and effect on porous structure of konjac
505 glucomannan-based aerogels. *International Journal of Biological*
506 *Macromolecules*, 92, 1130-1135.

507 Palumbo, M., Avellaneda, J., & Lacasta, A. M. (2015). Availability of crop
508 by-products in Spain: New raw materials for natural thermal insulation.
509 *Resources Conservation & Recycling*, 99, 1-6.

510 Ramírez-Villegas, R., Eriksson, O., & Olofsson, T. (2016). Assessment of renovation
511 measures for a dwelling area – Impacts on energy efficiency and building
512 certification. *Building and Environment*, 97, 26-33.

513 Randall, J. P., Meador, M. A., & Jana, S. C. (2011). Tailoring mechanical properties of
514 aerogels for aerospace applications. *ACS Applied Materials & Interfaces*, 3(3),
515 613.

516 Robitzer, M., Renzo, F. D., & Quignard, F. (2011). Natural materials with high surface
517 area. Physisorption methods for the characterization of the texture and surface
518 of polysaccharide aerogels. *Microporous & Mesoporous Materials*, 140(1–3),
519 9-16.

520 Sabri, F., Marchetta, J. G., Faysal, K. M. R., Brock, A., & Roan, E. (2014). Effect of
521 aerogel aarticle concentration on mechanical behavior of impregnated RTV
522 655 compound material for aerospace applications. *Advances in Materials*
523 *Science & Engineering*, 2014(14).

524 Septevani, A. A., Evans, D. A. C., Chaleat, C., Martin, D. J., & Annamalai, P. K.
525 (2015). A systematic study substituting polyether polyol with palm kernel oil
526 based polyester polyol in rigid polyurethane foam. *Industrial Crops and*

527 *Products*, 66, 16-26.

528 Shi, J., Lu, L., Guo, W., Zhang, J., & Cao, Y. (2013). Heat insulation performance,
529 mechanics and hydrophobic modification of cellulose–SiO₂ composite
530 aerogels. *Carbohydrate Polymers*, 98(1), 282-289.

531 Thakur, V. K., & Voicu, S. I. (2016). Recent advances in cellulose and chitosan based
532 membranes for water purification: A concise review. *Carbohydrate Polymers*,
533 146, 148-165.

534 Wang, J., Zhao, D., Shang, K., Wang, Y. T., Ye, D. D., Kang, A. H., Wang, Y. Z.
535 (2016). Ultrasoft gelatin aerogels for oil contaminant removal. *Journal of*
536 *Materials Chemistry A*, 4(24).

537 Wang, T., Sun, H., Long, J., Wang, Y., & Schiraldi, D. A. (2016). Biobased
538 poly(furfuryl alcohol)/clay aerogel composite prepared by a freeze drying
539 process. *Acs Sustainable Chemistry & Engineering*, 4(5).

540 Wang, X., Zhong, J., Wang, Y., & Yu, M. (2006). A study of the properties of carbon
541 foam reinforced by clay. *Carbon*, 44(8), 1560-1564.

542 Wang, Y., Alhassan, S. M., Yang, V. H., & Schiraldi, D. A. (2013).
543 Polyether-block-amide copolymer/clay films prepared via a freeze-drying
544 method. *Composites Part B: Engineering*, 45(1), 625-630.

545 Wang, Y., Chen, X., Kuang, Y., Jiang, F., & Yan, W. (2017). Progress in application of
546 polysaccharide aerogels. *Journal of Wuhan Institute of Technology*, 39(5),
547 443-449.

548 Wang, Y., Chen, X., Kuang, Y., Xiao, M., Su, Y., & Jiang, F. (2017). Microstructure
549 and filtration performance of konjac glucomannan-based aerogels
550 strengthened by wheat straw. *International Journal of Low-Carbon*
551 *Technologies*.

552

553

554

555

556

557

558

559

560

Supplementary data

[Click here to download Supplementary data: Supplementary material.docx](#)

